Mas, M. T., Resplandor, Z. E., & Riggs, A. D. (1987) *Biochemistry 26*, 5369-5372.
Mas, M. T., Bailey, J. M., & Resplandor, Z. E. (1988) *Biochemistry 27*, 1168-1172.
Pickover, C. A., McKay, D. B., Engelman, D. M., & Steitz, T. A. (1979) *J. Biol. Chem. 254*, 11323-11329.
Price, N. C., & Hunter, M. G. (1976) *Biochim. Biophys. Acta 445*, 364-376.
Rao, S. T., & Rossman, M. G. (1973) *J. Mol. Biol. 76*, 241-256.
Rossman, M. G., & Argus, P. (1981) *Annu. Rev. Biochem. 50*, 497-532.
Scopes, R. K. (1978) *Eur. J. Biochem. 85*, 503-516.
Snow, J. W., Brandts, J. F., & Low, P. S. (1978) *Biochim. Biophys. Acta 512*, 579-591.
Snow, J. W., Vincentelli, J., & Brandts, J. F. (1981) *Biochim. Biophys. Acta 642*, 418-428.
Sturtevant, J. M. (1987) *Annu. Rev. Phys. Chem. 38*, 463-488.
Subramani, S., & Schachman, H. K. (1980) *J. Biol. Chem. 255*, 8136-8143.
Watson, H. C., Walker, N. P. C., Shaw, P. J., Bryant, T. N., Wendell, P. L., Fothergill, L. A., Perkins, R. E., Conroy, S. C., Dobson, M. J., Thite, M. F., Kingsman, A. J., & Kingsman, S. M. (1982) *EMBO J. 1*, 1635-1640.
Wetlaufer, D. B. (1973) *Proc. Natl. Acad. Sci. U.S.A. 70*, 697-701.
Wetlaufer, D. B. (1981) *Adv. Protein Chem. 34*, 61-89.
Yue, R. H., Palmieri, R. H., Olson, O. E., & Kuby, S. A. (1967) *Biochemistry 6*, 3204-3227.

X-ray Studies of Aspartic Proteinase–Statine Inhibitor Complexes

J. B. Cooper, S. I. Foundling,‡ and T. L. Blundell*
Laboratory of Molecular Biology, Department of Crystallography, Birkbeck College, London WC1E 7HX, U.K.
J. Boger
Merck Sharp & Dohme Research Laboratories, Rahway, New Jersey 07065
R. A. Jupp and J. Kay
Department of Biochemistry, University College, Cardiff, Wales
Received January 17, 1989; Revised Manuscript Received May 4, 1989

ABSTRACT: The conformation of a statine-containing renin inhibitor complexed with the aspartic proteinase from the fungus *Endothia parasitica* (EC 3.4.23.6) has been determined by X-ray diffraction at 2.2-Å resolution (R = 0.17). We describe the structure of the complex at high resolution and compare this with a 3.0-Å resolution analysis of a bound inhibitor, L-364,099, containing a cyclohexylalanine analogue of statine. The inhibitors bind in extended conformations in the long active-site cleft, and the hydroxyl of the transition-state analogue, statine, interacts strongly with the catalytic aspartates via hydrogen bonds to the essential carboxyl groups. This work provides a detailed structural analysis of the role of statine in peptide inhibitors. It shows conclusively that statine should be considered a dipeptide analogue (occupying P_1 to P_1') despite lacking the equivalent of a P_1' side chain, although other inhibitor residues (especially P_2) may compensate by interacting at the unoccupied S_1' specificity subsite.

The aspartic proteinases are characterized by their dependence on two essential aspartic acid residues (32 and 215 in pepsin) and their susceptibility to inhibition by the microbial product pepstatin (Umezawa et al., 1970), which has an apparent K_i for pepsin of 5×10^{-11} M (Workman & Burkitt, 1979).

pepstatin: Ival-Val-Val-Sta-Ala-Sta

Pepstatin contains two residues of the rare amino acid statine [(4*S*,3*S*)-4-amino-3-hydroxy-6-methylheptanoic acid], the central statine being essential for potent inhibition (Rich et al., 1977, 1980; Rich & Bernatowicz, 1982).

Statine (with its leucyl-like side chain)

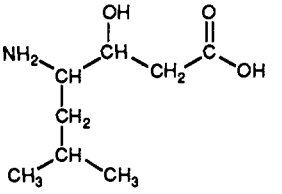

mimics the tetrahedral transition state or intermediate of peptide-bond hydrolysis [$-C(OH)_2NH-$]. In general, inhibitors having the R configuration at C-3 are significantly less potent than the S enantiomers (Rich et al., 1980; Liu et al., 1979), which indicates that the enzyme has a stereospecific binding site for the hydroxyl group. This was confirmed by X-ray crystallographic studies of complexes of fungal aspartic proteinases with pepstatin (James et al., 1982, 1985; Bott et al., 1982, 1983) which showed that the C-3 hydroxyl group is bound by a symmetrical hydrogen-bonding arrangement to the two essential carboxyl groups which probably share a single

* To whom correspondence should be addressed.
‡ Present address: E. I. du Pont de Nemours & Co., Inc., Central Research and Development, Bldg 328/350A, Experimental Station, Wilmington, DE 19898.

0006-2960/89/0428-8596$01.50/0

Table I: Sequences of the Inhibitors Compared with Human Angiotensinogen[a]

	P_6	P_5	P_4	P_3	P_2	P_1	P_1'	P_2'	P_3'
angiotensinogen	Ile	His	Pro	Phe	His	Leu	Val	Ile	His
L-363,564	Boc	His	Pro	Phe	His	Sta		Leu	Phe-NH_2
L-364,099	Iva	His	Pro	Phe	His	ACHPA		Leu	Phe-NH_2

[a] Sta, statine; ACHPA, 4-amino-5-cyclohexyl-3-hydroxypentanoic acid.

negative charge in the optimal pH range (Pearl & Blundell, 1984). The residues on the carboxy-terminal side of the statine were either absent or poorly defined in these earlier analyses. All residues of pepstatin contribute significantly to its potency (Marciniszyn et al., 1976; Rich et al., 1980; Rich & Salituro, 1983), suggesting that aspartic proteinases have extended binding clefts.

The inhibition of different aspartic proteinases by pepstatin is highly variable. For example, renin is inhibited relatively weakly (Boger et al., 1983). This led to the suggestion that it may be possible to optimize a statine inhibitor for a specific enzyme by altering the neighboring sequence (Marciniszyn et al., 1976).

Inhibition of the plasma proteinase renin has been shown to lower blood pressure in humans by depressing angiotensin II levels and may be useful in the treatment of hypertension (Leckie, 1985; Webb et al., 1983). L-363,564, a statyl peptide based on the renin substrate angiotensinogen (Table I), is a potent and selective renin inhibitor (Boger et al., 1983, 1985). To understand the binding of such inhibitors to aspartic proteinases, we have cocrystallized L-363,564 with the aspartic proteinase from the fungus *Endothia parasitica* (endothiapepsin) with a view to a high-resolution study using X-ray diffraction. We have also cocrystallized endothiapepsin with a more potent renin inhibitor, L-364,099 (Boger et al., 1985b) (Table I), in which the leucine-like side chain of the statine has been substituted with the cyclohexylalanine analogue.

An X-ray analysis at 2.1-Å resolution (R value = 0.16) shows that the 330 residues of endothiapepsin lie predominantly in β-sheets forming two lobes that are topologically related by a pseudo 2-fold axis (Blundell et al., 1985). Similar structures are found for other aspartic proteinases, for example, pepsinogen (James & Sielecki, 1986) and human renin (Sielecki et al., 1989). Evolution, by gene multiplication, from a primordial monomeric or dimeric proteinase has been suggested due to the structural similarity of both domains (13 of the 86 topologically related residues are identical in endothiapepsin) (Tang et al., 1978). The structural similarity is greatest at the active center between the two domains, where a network of hydrogen bonds restrain the essential carboxyl groups to be in close proximity and approximately coplanar (Pearl & Blundell, 1984). The primary specificity pockets, S_1 and and S_1' [nomenclature of Berger and Schechter (1970)] next to the aspartates, are predominantly hydrophobic.

The L-363,564 cocrystals, grown close to the optimal pH of the enzyme, are isomorphous with those of native endothiapepsin. The bound structure of L-363,564 has been solved to 2.2-Å resolution with a crystallographic agreement (R) value of 0.17, and a preliminary paper has been published (Foundling et al., 1987). The L-364,099 cocrystals were nonisomorphous but grew with the same unit cell as another inhibitor cocrystal (BW625) that had already been solved by molecular replacement. This has allowed the L-364,099 structure to be solved by the difference Fourier method and compared with the L-363,564 structure. In this paper the L-363,564 structure is described in detail, and its relevance to the mechanism and inhibition of aspartic proteinases is discussed. The paper provides a detailed structural analysis of the role of statine in peptide inhibitors and shows conclusively that it should be considered a dipeptide analogue.

Table II: Unit Cell Parameters of Native and Inhibitor Crystals ($P2_1$)

	a	b	c	β (deg)
endothiapepsin	53.6	74.1	45.7	110.0
L-363,564 complex	53.5	73.9	45.6	109.1
L-364,099 complex	43.0	75.8	42.8	97.0

X-RAY ANALYSIS

Cocrystals of endothiapepsin and the inhibitors were grown in 0.1 M acetate buffer at pH 4.6 by adapting the method of Moews and Bunn (1970). Lyophilized endothiapepsin and a 10-fold molar excess of inhibitor were slowly dissolved to give a 2 mg/mL enzyme solution, and ammonium sulfate was added in stages to 55% saturation (2.2 M). After millipore filtration, a few drops of acetone were added to the mother liquor. The L-363,564 crystals were grown in 2-mL batches and took 12 months to achieve a size suitable for diffractometer data collection. These cocrystals were isomorphous with the native enzyme which crystallizes in space group $P2_1$. The significant difference in β angle (0.9°) between native and complex crystals (Table II) as well as small intensity changes observed in precession photographs indicated that the inhibitor had cocrystallized with the enzyme. Reflections in the 15–2.2-Å range were measured with Hilger and Watts Y290 and Enraf-Nonius CAD4F diffractometers using four crystals. A total of 27 112 reflections were recorded and corrected for Lorentz polarization, resolution-dependent fading, and absorption (North et al., 1968) prior to merging (Rae, 1965; Rae & Blake, 1966), which gave a unique set of 15 553 reflections with $F \geq 1\sigma(F)$, $R = 0.04$. This represents 95% of the data in the measured range, and 71% of it is more significant than $3\sigma(I)$. The first data set collected (2.6 Å) was used to calculate difference Fouriers, $|F_{PI}| - |F_P|$ and $2|F_{PI}| - |F_P|$, with the refined phases of the native enzyme. These maps were displayed on an Evans and Sutherland PS2 using the program FRODO (Jones, 1978) as modified by Dr. I. J. Tickle. A stretch of contiguous density in the active-site cleft was apparent, the strongest feature being 7 times the RMS density of the $|F_{PI}| - |F_P|$ map. The density defined the conformation of the inhibitor from P_4 to P_2', and the coordinates obtained by fitting were subjected to least-squares refinement using the program RESTRAIN (Moss & Morffew, 1982; Haneef et al., 1985). The rigid body refinement option was used with the medium-resolution data to compensate for the difference in β angle of the inhibitor cocrystals. Subsequently, all atomic coordinates and isotropic temperature factors were refined by gradual inclusion of the high-resolution reflections. After 18 cycles, "omit" maps were calculated at 2.2 Å by using $m|F_o| - D|F_c|$ and $2m|F_o| - D|F_c|$ as coefficients [see Read (1986) for explanation] to identify the P_6, P_5, and P_3' residues. However, the electron density for the P_3' Phe remained unsatisfactory. This residue was eventually placed in a position of reasonable geometry, and the complex was subjected to a further eight cycles of refinement, leading to an R factor of 0.18. The density for P_3' Phe was not improved, and so this residue was not included

Table III: Refinement Statistics for the L-363,564 Complex

RMS deviation from target bond distances (Å)	0.014
RMS deviation from target angle distances (Å)	0.018
RMS deviation from minimum nonbonded contact distance (Å)	0.021
RMS distance from least-squares main-chain planes (Å)	0.002
RMS distance from least-squares side-chain planes (Å)	0.002

resolution range (Å)	*R* factor	no. of reflections
10–3.9	0.17	2835
3.9–3.1	0.14	2808
3.1–2.8	0.17	2766
2.8–2.5	0.18	2554
2.5–2.3	0.20	2169
2.3–2.2	0.23	2290

mean U_{ios} for 2389 enzyme atoms (Å^2)	0.232
mean U_{iso} for 65 inhibitor atoms (Å^2)	0.371
mean U_{iso} for 321 waters (Å^2)	0.552

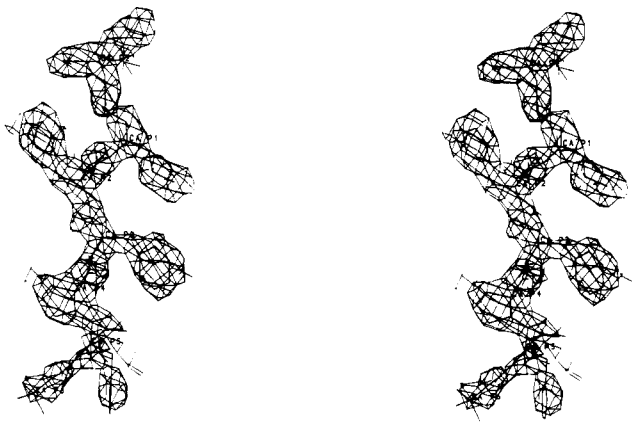

FIGURE 1: $2F_o - F_c$ electron density map at 2.2 Å for L-363,564 showing the polypeptide from P_6 to P_2' in stereo.

in the subsequent analysis. After rebuilding, the group occupancy of the inhibitor (P_6 to P_2') was refined for a further six cycles, giving a value of 89%. The *R* value is 0.172 for data between 10 and 2.2 Å [$F \geq 1\sigma(F)$]; 321 waters were included in the refinement. More refinement statistics are given in Table III, and the electron density for the inhibitor (P_6–P_2') is shown in Figure 1. The RMS coordinate error for the whole complex, calculated from Read (1986), is 0.21 Å.

Small cocrystals of L-364,099 cocrystals grew under the same conditions after 3 years. These crystals were monoclinic $P2_1$ but were not isomorphous with the native enzyme (Table II). Only one small crystal was suitable for data collection that proceeded to 3.0 Å by using a CAD4F diffractometer and gave 5548 reflections that were reduced to 4993 uniques with a merging *R* value of 0.11. Of this data 83% is more significant than $3\sigma(I)$. The same crystal habit had been obtained before with another inhibitor (BW625), the analysis of which will be described in more detail elsewhere. The orientation of the enzyme in the BW625 unit cell was determined previously by using the cross-rotation function (Crowther, 1972) with 2.9-Å data which produced a peak 17 times the RMS value. The position of the enzyme relative to the 2-fold screw axis was then found by calculating the T_2 function (Crowther & Blow, 1962; Tickle, 1985) for the *XZ* plane which contained a peak 16 times the RMS value. The molecular replacement solution of BW625 was optimized by rigid body (2.9 Å) followed by restrained refinement at 2.2 Å. The resulting coordinates were used to calculate phases for the enzyme in the new unit cell. These together with the 3.0-Å resolution L-364,099 data were used to calculate a difference Fourier map (with coefficients $|F_o| - |F_c|$) that showed good density for the inhibitor from P_6 to P_2'. The resulting model was subjected

Table IV: Refinement Statistics for the L-364,099 Complex

RMS deviation from target bond distances (Å)	0.015
RMS deviation from target angle distances (Å)	0.028
RMS deviation from minimum nonbonded contact distance (Å)	0.052
RMS distance from least-squares main-chain planes (Å)	0.019
RMS distance from least-squares side-chain planes (Å)	0.004

resolution range (Å)	*R* factor	no. of reflections
10–5.2	0.25	802
5.2–4.2	0.23	808
4.2–3.8	0.28	813
3.8–3.4	0.30	816
3.4–3.2	0.33	772
3.2–3.0	0.32	752

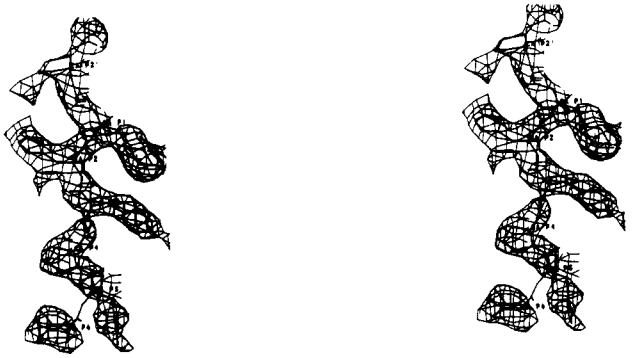

FIGURE 2: Part of the $2F_o - F_c$ map at 3.0 Å for L-364,099 showing from P_6 to P_2' in stereo.

to three cycles of restrained refinement followed by rebuilding and further refinement (four cycles). The resulting *R* factor was 0.28 for data between 10 and 3.0 Å [$F \geq 1\sigma(F)$]. No water molecules were included, and the occupancy was not refined. The $2F_o - F_c$ map for the inhibitor is shown in Figure 2, and refinement statistics are given in Table IV.

Results and Discussion

The electron density map for L-363,564 at 2.2 Å (Figure 1) is contiguous from P_6 to P_2', although the inner residues (P_4–P_1) are most clearly defined (see Table III). In the medium-resolution map for L-364,099 (3.0 Å), density is present from P_6 to P_2'. The interpretation of the original difference map for L-364,099 depended heavily on the refined L-363,564 structure.

L-363,564 lies in an extended conformation along the active-site cleft, shown in Figures 3 and 4, running approximately antiparallel with a β-strand from Gly 217 to Leu 220. The residues of this strand make a number of hydrogen bonds to the main chain of each inhibitor from P_3 to P_1. The active site "flap" (Trp 71–Gly 82) lies over the P_2, P_1–P_1', and P_2' residues and forms several van der Waals contacts and hydrogen bonds with the inhibitors. At S_1 the statine hydroxyl is within hydrogen-bonding distance of and approximately coplanar with both essential carboxyl groups (32 and 215). The carboxy-terminal side of the inhibitor curls out from beneath the flap and is partly exposed to solvent. The conformation adopted by L-364,099 appears identical with that of L-363,564 within the errors of the analysis (e.g., compare Figures 1 and 2).

The main chains of both inhibitors make a total of 10 possible hydrogen-bonding contacts with the enzyme, shown schematically in Figure 5 for L-363,564. The statine carbonyl makes a hydrogen bond with the main-chain nitrogen of Gly 76. This hydrogen bond has been seen in several other inhibitor complexes [e.g., see Foundling et al. (1987)] but usually involves the P_1' carbonyl, which indicates that statine is a dipeptide analogue, spanning the S_1 and S_1' regions, due to the extra main-chain atoms. In addition, the P_1' Cα of reduced

Table V: Details of the L-363,564 Binding Subsites (Where Different, the Data for L-64,099 Are Shown in Parentheses)

position	P_6	P_5	P_4	P_3	P_2	P_1	P_1'	P_2'	P_3'
residue	Boc (Ival)	His	Pro	Phe	His	Sta (ACHPA)		Leu	Phe-NH_2
quality of electron density	weak	weak	good	good	good	good		good	weak
no. of van der Waals contacts ($d \leq 4.0$ Å)	10 (7)	19 (16)	10 (4)	33 (24)	26 (22)	45 (49)		10 (6)	
no. of hydrogen-bond contacts distances ($d \leq 3.3$ Å)	0	0	0	2	1	6[a]		1	

[a] The C-3 hydroxyl of this residue is within hydrogen-bonding distance of all four carboxyl oxygens of aspartates 32 and 215, although at any one time probably only two hydrogen bonds are formed.

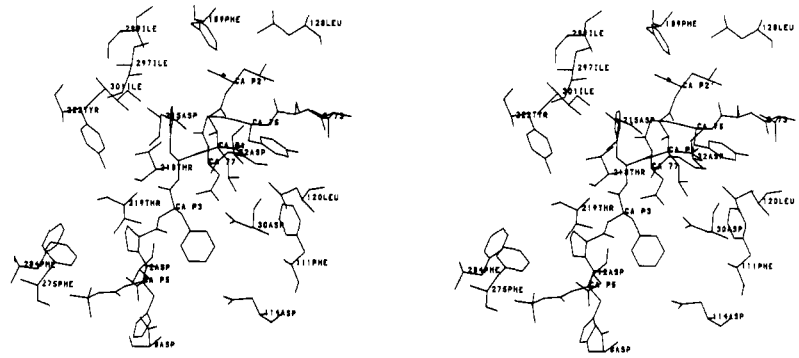

FIGURE 3: Stereoview of L-363,564 and the active-site-cleft residues of endothiapepsin.

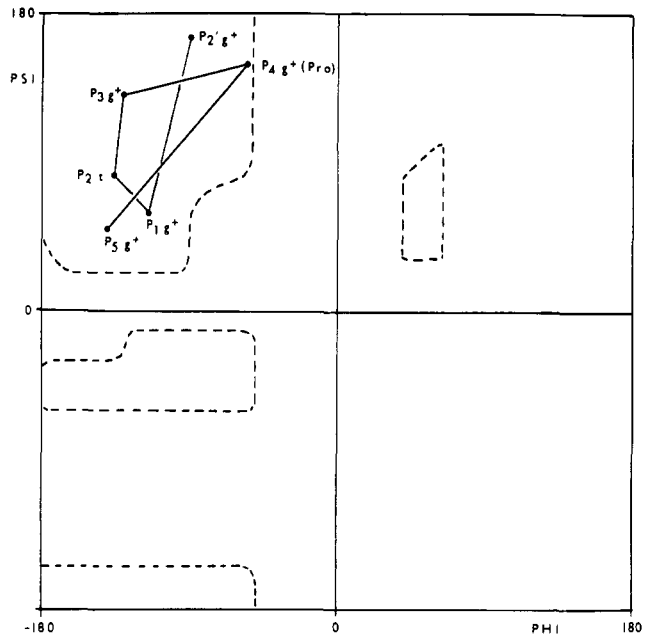

FIGURE 4: Ramamchandran plot showing the conformation of L-363,564. Side-chain conformations (χ_1 angles) are shown by using the notation of Janin et al. (1978).

bond inhibitors ($-CH_2NH-$) lies close (0.79 Å) to the position occupied by the main-chain methylene at P_1 of L-363,564 (Foundling et al., 1987). Further evidence is provided by the residue following the statine that occupies the same subsite as the P_2' residue in reduced bond inhibitor complexes.

The P_2 carbonyl also forms a hydrogen bond to the peptide nitrogen of another flap residue, Asp 77. In human renin the β-hairpin residues, Gly 76 and Asp 77, are replaced by Ser and Thr, respectively [alignment from Sibanda et al. (1984)]. These changes, coupled with the deletion at position 81, imply that interactions with the flap may be slightly different in renin. In the 24 known aspartic proteinase sequences there are 10 absolutely conserved glycine residues (J. Overington, unpublished work). Two of these, 34 and 217, appear to accept hydrogen bonds from the inhibitor main chain at P_2' and P_1, respectively. These glycines also allow the main chain of the

Table VI: Residues Forming the Binding Pockets of Endothiapepsin As Defined by Interaction with L-363,564 (Contacts ≤4.0Å)[a]

S_6	Pro 3	Phe 275	Gly 276	Pro 277	Phe 284
	W373				
S_5	Asp 8	Asp 12			
S_4	Asp 12	Thr 219	W202	W244	W106
S_3	Asp 12	Ala 13	Asp 114	Gly 217	Thr 218
	Thr 219	W106	W108	W150	W200
S_2	Tyr 75	Gly 76	Asp77	Thr 218	Ile 297
	Ile 301				
S_1–S_1'	Asp 30	Asp 32	Gly 34	Tyr 75	Gly 76
	Asp 77	Leu 120	Asp 215	Gly 217	Thr 218
S_2'	Gly 34	Ile 73	Ser 74	Gly 76	Leu 128
	Phe 189				

[a] Water molecules that participate in binding are prefixed by W.

enzyme following both aspartates to fold sharply so that the hydroxylic side chains at 35 and 218 (Ser and Thr, respectively, in endothiapepsin) can interact with the essential carboxyl groups (Pearl & Blundell, 1984). The threonine residue at 219 makes two good hydrogen bonds with the inhibitor main chain at P_3. The carbonyl at P_3 accepts a hydrogen bond from the amide nitrogen of 219, and the γ-hydroxyl oxygen of this residue accepts a hydrogen bond from the P_3 nitrogen. Residue 219 is a serine in human renin, and hence both of these hydrogen bonds are likely to be conserved. All of these interactions are probably important for productive binding of substrates. The presence of two hydroxylic residues in the renin flap (Ser 76 and Thr 77) may allow additional or alternative hydrogen-bonding interactions with a substrate peptide. A summary of the interactions between the enzyme and L-363,564 is given in Table V, and the residues that line the binding subsites are listed in Table VI. There appears to be one hydrogen bond to the enzyme involving a water molecule (W106) which is 2.8 Å from the carbonyl of P_3 and within hydrogen-bonding distance of both the hydroxyl of Tyr 222 and the NH of Leu 220.

The S_6 pocket is contiguous with S_4 and is lined with several aromatic residues, e.g., Phe 284 and Phe 275, which interact with the hydrophobic *tert*-butyloxycarbonyl group (Boc) of L-363,564 and the isovaleryl group of L-364,099. The main-chain atoms of the Boc blocking group [C-$(Me)_3OCONHC\alpha$] at P_6 of L-363,564 appear to be approx-

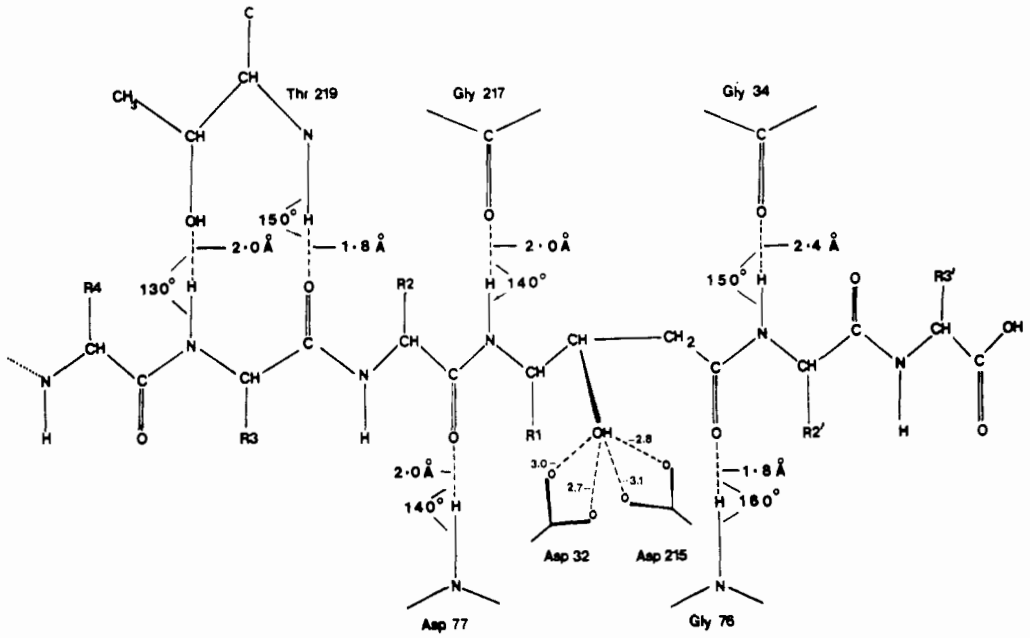

FIGURE 5: Schematic diagram of hydrogen bonds to L-363,564.

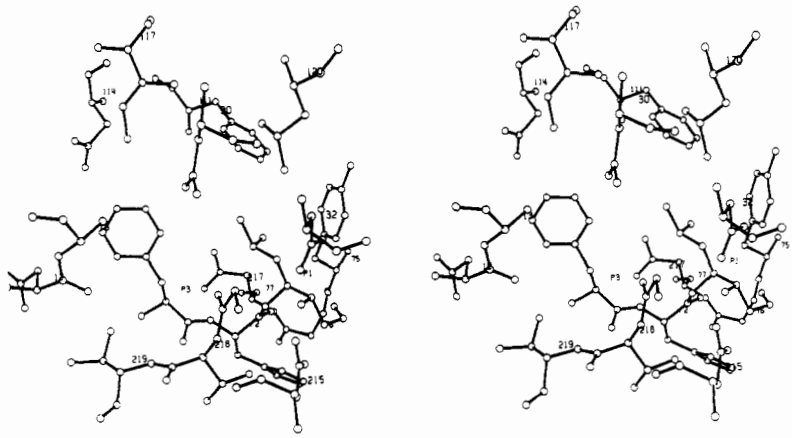

FIGURE 6: Stereoview showing residues of the S_3–S_1 pockets. Note aspartates 32 and 215 interacting with the P_1 hydroxyl of L-363,564.

imately coplanar. This is consistent with several small molecule structures [e.g., Singh et al. (1987)] and is probably due to delocalization of electrons over the ester as well as the amide moieties. The S_5 pocket that lies on the surface of the N-terminal domain is more polar than S_6 and contains several carboxyl groups, e.g., Asp 12 and Asp 8, which may interact electrostatically with the P_5 histidines of both inhibitors. The Nδ1 of His P_5 of L-363,564 is 3.4 Å from one carboxyl oxygen of Asp 12, thereby forming a weak, although possibly charge-assisted, hydrogen bond.

Replacing the phenylalanine at P_3 of a renin inhibitor with alanine reduced the potency of the inhibitor 4000-fold (Boger, 1985). Hence, this residue must make a large contribution to inhibitory potency. The aromatic ring makes van der Waals contact with Ile 117, Ala 13, and three aspartate carboxyls, namely, 12, 30, and 114, which are presumably protonated in the complex. The equivalent residues of human renin are Thr, Val, and Ala [alignment from Sibanda et al. (1984)], which provide a larger and more hydrophobic pocket. The Phe to Ala change was found to have a smaller effect on fungal aspartic proteinases presumably because the pocket is more hydrophilic in these enzymes. The phenylalanine ring also makes contact with a bound solvent (W108) lying between the contiguous S_1 and S_3 pockets. The electron density for this water is elongated, indicating static or dynamic disorder. The side chain of Asp 77 lies over the S_3 and S_1 pockets. It has been shown to interact via a hydrogen bond with the ζ-amino group of a lysine at P_1 of a modified statine (LySta) inhibitor (James et al., 1985; Salituro et al., 1987).

The S_2 subsite of endothiapepsin is large and exposed to solvent, allowing inhibitor side chains to adopt different orientations in the pocket (Foundling et al., 1987). The imidazole side chain at P_2 of both inhibitors is oriented toward the S_1' subsite and lies in a position surrounded by several hydrophobic residues: Tyr 222, Ile 301, and Ile 297. In the model of human renin the corresponding residues are Ser, Ala, and Gly, which would provide a more polar environment for the histidine of angiotensinogen. However, the conformation of this part of the renin structure may be different due to the insertion of a proline-rich sequence at position 294 (Sibanda et al., 1984). With endothiapepsin complexes markedly different inhibitor side-chain conformations are seen at P_2; e.g., the P_2 histidine of the reduced-bond analogue H-142 (Szelke et al., 1982) is oriented away from the S_1' region toward the side chain of Asp 77. In contrast, the P_2 His residues of L-363,564 and L-364,099 partially occupy the S_1' pocket left empty by the statine residue that lacks a P_1' side chain.

In addition to the tight binding of the C-3 hydroxyl to the essential carboxyls, the leucine-like side chain at P_1 of L-363,564 makes van der Waals contact with several residues

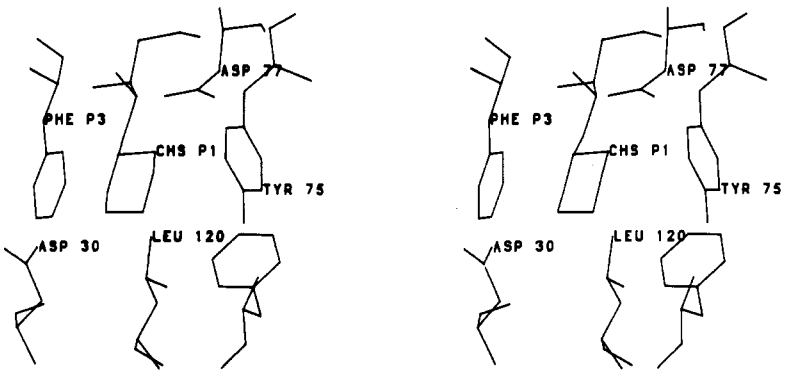

FIGURE 7: Stereoview showing the P_1 cyclohexyl analogue of statine and the residues of the S_1 pocket.

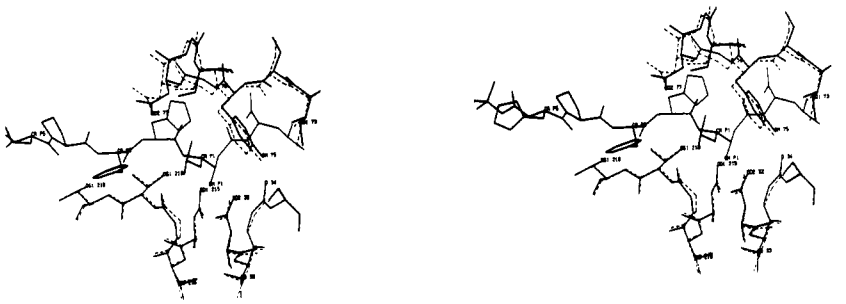

FIGURE 8: Stereoview of the active-site residues with L-363,564. The dashed lines represent the native enzyme, indicating small conformational changes.

of the N-terminal lobe: Tyr 75 of the active-site flap, Leu 120, and Asp 30 (Figure 6). Examination of both the 3.0-Å L-364,099 electron density at high contour level and possible steric clashes indicates that the cyclohexylalanine side chain is probably in a chair conformation, allowing it to interact with the same set of residues as statine but to make more extensive van der Waals contacts (Figure 7) especially with Phe 111. The S_1 residues are conserved in human renin except for Leu 120 and Asp 30, which are both valines. Hence, in renin the S_1 pocket would appear to be more hydrophobic than in endothiapepsin. These predictions are not inconsistent with the crystallographic analysis of human renin (Sielecki et al., 1989).

L-364,099 inhibits human renin with a K_i value of 0.16 nM (Table VII), making it at least 10-fold more potent than L-363,564 (K_i = 2.3 nM). This difference may be due largely to the different number of interactions at P_1. The difference in van der Waals contact area between the statine and cyclohexylstatine residues of the two inhibitor structures, calculated by using MS (Connolly, 1983), is 29 Å^2. Assuming that most of the difference in binding energy between these two inhibitors is due to the P_1 residues, the corresponding free energy difference is about 12 kJ mol^{-1} (Richards & Richmond, 1978). This corresponds to a ratio in binding constant of 120, which is in accordance with the K_i values. The endothiapepsin-bound structure of another inhibitor solved at high resolution (1.8 Å) revealed that a cyclohexyl side chain at P_1 forces the phenyl ring at P_3 to adopt an unfavorable χ_2 angle (A. Sali, unpublished results) as appears to be the case for L-364,099 (Figure 2). This is consistent with the K_i data in Table VII which show that a cyclohexyl side chain at P_1 has a detrimental effect on the potency for most aspartic proteinases including endothiapepsin, the exception being human renin. The different shapes of the S_1 and S_3 pockets of renin may allow large cyclic side chains to be accommodated without unfavorable interactions. Selective inhibition of renin can therefore be achieved.

The hydrogen bonds to the inhibitor involving the conserved glycines at 34 and 217 appear to be weaker in the L-363,564 complex than in the reduced-bond inhibitor (–CH_2NH–) complexes (Cooper et al., 1987). This may be due to the differences in main-chain length of each analogue and their different interactions with the aspartate diad. The NH group of a reduced-bond analogue may be protonated and could interact electrostatically with the aspartate carboxyls, whereas the C-3 hydroxyl of statine (–CHOHCH_2–) has been shown to lie in the plane of the diad. Hence there appears to be a local frameshift of approximately one bond length between reduced-bond and statine inhibitors (Foundling et al., 1987).

Table VII: Inhibition Constants (K_i) for Interaction of L-363,564 and L-364,099 with a Variety of Aspartic Proteinases[a]

enzyme	K_i (nM)	
	L-363,564	L-364,099
human renin	2.3	0.16
human pepsin	1000	2200
human gastricsin	440	860
human cathepsin D	70	230
human cathepsin E	8	60
endothiaproteinase	40	420

[a] Assays were carried out at 37 °C at pH 3.1 and anionic strength of 0.1 M by using synthetic chromogenic peptide substrates except for the human renin. These assays were performed at pH 7.2 by using angiotensinogen as substrate and measurement of the angiotensin I released by immunoassay.

The leucine following the statine lies in the S_2' pocket that is formed by Leu 128, Phe 189, and the main chain of the flap. Electron density for the P_3' phenylalanine and the C-terminal amide group of L-363,564 is absent, which indicates that this part of the inhibitor may be disordered or mobile or may have been cleaved by the enzyme. The latter might be possible in view of the long crystallization period and the specificity of the enzyme for hydrophobic and especially aromatic groups (Cooper et al., 1987; Dunn et al., 1986, 1987).

Strong contiguous features of positive $F_{PI} - F_P$ electron density in the 2.6-Å difference map of L-363,564 corresponding to the active-site flap indicated that these residues may become more ordered on complex formation. The re-

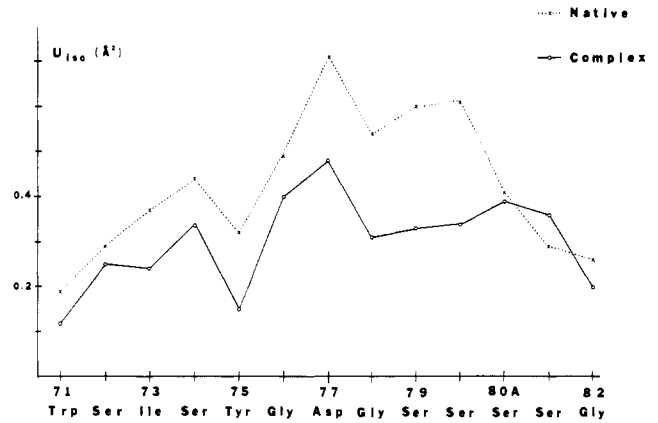

FIGURE 9: Average isotropic temperature factors for residues of the active-site flap of the native enzyme and L-363,564 complex.

finement has shown that the conformation of the flap does not change much when an inhibitor binds (Figure 8). The nearly identical resolution ranges used in refinement of the native enzyme and L-363,564 complex (10–2.1 and 10–2.2 Å, respectively) enable the isotropic temperature factors of both forms to be compared. The largest differences are found in the flap which has lower temperature factors in the inhibitor complex (Figure 9). This has been observed for penicillopepsin and rhizopuspepsin inhibitor complexes (James et al., 1985; Suguna et al., 1987) and is consistent with the hydrogen bonds and van der Waals interactions between the enzyme and the inhibitor and may account for the difference density surrounding the flap in the original difference map.

L-363,564 replaces 18 solvent molecules that are present in the active-site cleft of the enzyme, including the water or cation that lies between the essential carboxyl groups.

The aspartic proteinase mechanism is considered to involve nucleophilic attack of a solvent molecule on the carbonyl group of the scissile bond (James & Sielecki, 1985; Pearl, 1987; Polgar, 1987; Suguna et al., 1987; Blundell et al., 1987). It is unknown if the C-3 hydroxyl of the statine is equivalent to the oxygen derived from the attacking nucleophile or the carbonyl oxygen of the substrate. Nevertheless, the bound structure of the inhibitor indicates that one oxygen of the intermediate is tightly bound to the aspartate diad. Using the bound structures of this and other transition-state analogues, we have speculated that the other oxygen of the intermediate (–OH or $-O^-$) will interact with the edge of the phenol ring of tyrosine 75 (Blundell et al., 1987) which resides in the loop over the active site. Edgewise interactions between buried oxygens and aromatic rings are favorable due to the partial positive charge at the edge of the ring and may contribute to the stability of protein structures (Thomas et al., 1982). A possible hydrogen-bond donor to the oxyanion is the Oγ of Ser 35, which is normally engaged in a hydrogen bond to the outer carboxyl oxygen of Asp 32. The positions of hydrogen atoms around the catalytic diad cannot be defined by X-ray analysis, and the sequence of proton transfers leading to cleavage of the peptide bond is unknown. However, the inhibitor structures have defined the set of residues that accommodate the tetrahedral intermediate of hydrolysis.

Registry No. Renin, 9015-94-5; pepsin, 9001-75-6; gastricsin, 9012-71-9; cathepsin D, 9025-26-7; cathepsin E, 110910-42-4; aspartic proteinase, 78169-47-8.

REFERENCES

Berger, A., & Schechter, I. (1970) *Philos. Trans. R. Soc. B257*, 249–264.

Blundell, T. L., Sibanda, B. L., & Pearl, L. H. (1983) *Nature 304*, 273–275.

Blundell, T. L., Jenkins, J., Pearl, L., Sewell, T., & Pederson, V. (1985) in *Aspartic proteinases and their inhibitors* (Kostka, V., Ed.) pp 151–161, de Gruyter, Berlin.

Blundell, T. L., Cooper, J., Foundling, S. I., Jones, D. M., Atrash, B., & Szelke, M. (1987) *Biochemistry 26*, 5585–5590.

Boger, J. (1985) in *Aspartic proteinases and their inhibitors* (Kostka, V., Ed.) pp 401–420, de Gruyter, Berlin.

Boger, J., Lohr, N. S., Ulm, E. H., Poe, M., Blaine, E. H., Fanelli, G. M., Lin, T.-Y., Payne, L. S., Schorn, T. W., Lamont, B. I., Vassil, T. C., Stabilito, I. I., Veber, D. F., Rich, D. H., & Bopari, A. S. (1983) *Nature 303*, 81–84.

Boger, J., Payne, L. S., Perlow, D. S., Lohr, N. S., Poe, M., Blaine, E. H., Ulm, E. H., Schorn, T. W., LaMont, B. I., Lin, T.-Y., Kawai, M., Rich, D. H., & Veber, D. F. (1985) *J. Med. Chem. 28*, 1779–1790.

Bott, R., & Davies, D. R. (1983) *Pept.: Struct. Funct., Proc. Am. Pept. Symp., 8th, 1983*, 531–540.

Bott, R., Subramanian, E., & Davies, D. R. (1982) *Biochemistry 21*, 6956–6962.

Connolly, M. L. (1983) *J. Appl. Crystallogr. 16*, 548–558.

Cooper, J. B., Foundling, S. I., Hemmings, A. M., Blundell, T. L., Jones, D. M., Hallett, A., & Szelke, M. (1987) *Eur. J. Biochem. 169*, 215–221.

Crowther, R. A. (1972) in *The molecular replacement method* (Rossmann, M. G., Ed.) pp 173–178, Gordon & Breach, New York.

Crowther, R. A., & Blow, D. M. (1962) *Acta Crystallogr. 15*, 544–548.

Dunn, B. M., Jimenez, M., Parten, B. F., Valler, M. J., Rolph, C. E., & Kay, J. (1986) *Biochem. J. 237*, 899–906.

Dunn, B. M., Valler, M. J., Rolph, C. E., Foundling, S. I., Jimenez, M., & Kay, J. (1987) *Biochim. Biophys. Acta 913*, 122–130.

Foundling, S. I., Cooper, J., Watson, F. E., Cleasby, A., Pearl, L. H., Sibanda, B. L., Hemmings, A., Wood, S. P., Blundell, T. L., Valler, M. J., Norey, C. G., Kay, J., Boger, J., Dunn, B. M., Leckie, B. J., Jones, D. M., Atrash, B., Hallett, A., & Szelke, M. (1987) *Nature 327*, 349–352.

Haneef, I., Moss, D. S., Stanford, M. J., & Borkakoti, N. (1985) *Acta Crystallogr. A41*, 426–433.

James, M. N. G., & Sielecki, A. R. (1985) *Biochemistry 24*, 3701–3713.

James, M. N. G., & Sielecki, A. R. (1986) *Nature 319*, 33–38.

James, M. N. G., Sielecki, A. R., Salituro, F., Rich, D. H., & Hofmann, T. (1982) *Proc. Natl. Acad. Sci. U.S.A. 79*, 6137–6142.

James, M. N. G., Sielecki, A. R., & Hofmann, T. (1985) in *Aspartic proteinases and their inhibitors* (Kostka, V., Ed.) pp 163–177, de Gruyter, Berlin.

Janin, J., Wodak, S., Levitt, M., & Maigret, B. (1978) *J. Mol. Biol. 125*, 357–386.

Jones, T. A. (1978) *J. Appl. Crystallogr. 11*, 268–272.

Leckie, B. J. (1985) in *Aspartic proteinases and their inhibitors* (Kostka, V., Ed.) pp 443–461, de Gruyter, Berlin.

Liu, W. S., Smith, S. C., & Glover, G. I. (1979) *J. Med. Chem. 22*, 577–579.

Marciniszyn, J., Hartsuck, J. A., & Tang, J. (1976) *J. Biol. Chem. 251*, 7088–7094.

Moews, P. C., & Bunn, C. W. (1970) *J. Mol. Biol. 54*, 395–397.

Moss, D. S., & Morffew, A. J. (1982) *Comput. Chem. 6*, 1–3.

North, A. C. T., Phillips, D. C., & Mathews, F. S. (1968) *Acta Crystallogr. A24*, 351–359.
Pearl, L. H. (1987) *FEBS Lett. 214*, 8–12.
Pearl, L. H., & Blundell, T. L. (1984) *FEBS Lett. 174*, 96–101.
Polgar, L. (1987) *FEBS Lett. 219*, 1–4.
Rae, A. D. (1965) *Acta Crystallogr. 19*, 683–684.
Rae, A. D., & Blake, A. B. (1966) *Acta Crystallogr. 20*, 586.
Read, R. J. (1986) *Acta Crystallogr. A42*, 140–149.
Rich, D. H., & Bernatowicz, M. S. (1982) *J. Med. Chem. 25*, 791–795.
Rich, D. H., & Salituro, F. G. (1983) *J. Med. Chem. 26*, 904–910.
Rich, D. H., Sun, E., & Singh, J. (1977) *Biochem. Biophys. Res. Commun. 74*, 762–767.
Rich, D. H., Sun, E. T. O., & Ulm, E. (1980) *J. Med. Chem. 23*, 27–33.
Richards, F. M., & Richmond, T. (1978) *J. Mol. Biol. 119*, 537–555.
Salituro, F. G., Agarwal, N., Hofmann, T., & Rich, D. H. (1987) *J. Med. Chem. 30*, 286–295.
Sibanda, B. L., Blundell, T. L., Hobart, P. M., Fogliano, M., Bindra, J. S., Dominy, B. W., & Chirgwin, J. M. (1984) *FEBS Lett. 174*, 102–111.
Sielecki, A. R., Hayakawa, K., Fujinaka, M., Murphy, M. E. P., Fraser, M., Muir, A. K., Carilli, C. T., Lewicki, J. A., Baxter, J. D., & James, M. N. G. (1989) *Science 243*, 1346–1351.
Singh, T. P., Haridas, M., Chauhan, V. S., & Kumar, A. (1987) *Biopolymers 26*, 819–829.
Suguna, K., Padlam, E. A., Smith, C. W., Carlson, W. D., & Davies, D. R. (1987) *Proc. Natl. Acad. Sci. U.S.A. 84*, 7009–7013.
Tang, J., James, M. N. G., Hsu, I. N., Jenkins, J. A., & Blundell, T. L. (1978) *Nature 271*, 618–621.
Thomas, K. A., Smith, G. M., Thomas, T. B., & Feldmann, R. J. (1982) *Proc. Natl. Acad. Sci. U.S.A. 79*, 4843–4847.
Tickle, I. J. (1985) in *Molecular replacement, proceedings of the Daresbury study weekend* (Machin, P., Ed.) DL/SCI/R23, pp 22–26, SERC, Daresbury Laboratory, U.K.
Umezawa, H., Aoyagi, T., Morishima, M., Matsuzaki, M., Hamada, M., & Takeuchi, T. (1970) *J. Antibiot. 23*, 259–261.
Webb, D. J., Cumming, A. M. M., Leckie, B. J., Lever, A. F., Morton, J. J., Robertson, J. I. S., Szelke, M., & Donovan, B. (1983) *Lancet ii*, 1486–1487.
Workman, R. J., & Burkitt, D. W. (1979) *Arch. Biochem. Biophys. 194*, 157–164.

Ruthenium–Iron Hybrid Hemoglobins as a Model for Partially Liganded Hemoglobin: Oxygen Equilibrium Curves and Resonance Raman Spectra†

Koichiro Ishimori,‡ Antonio Tsuneshige,§ Kiyohiro Imai,§ and Isao Morishima*,‡
Division of Molecular Engineering, Graduate School of Engineering, Kyoto University, Kyoto 606, Japan, and Department of Physicochemical Physiology, Medical School, Osaka University, Osaka 530, Japan
Received March 16, 1989; Revised Manuscript Received June 14, 1989

ABSTRACT: The structure and function of iron(II)–ruthenium(II) hybrid hemoglobins $\alpha(Ru\text{-}CO)_2\beta(Fe)_2$ and $\alpha(Fe)_2\beta(Ru\text{-}CO)_2$, which can serve as models for the intermediate species of the oxygenation step in native human adult hemoglobin, were investigated by measuring oxygen equilibrium curves and the Fe(II)–N_ϵ (His F8) stretching resonance Raman lines. The oxygen equilibrium properties indicated that these iron–ruthenium hybrid hemoglobins are good models for the half-liganded hemoglobin. The pH dependence of the oxygen binding properties and the resonance Raman line revealed that the quaternary and tertiary structural transition was induced by pH changes. When the pH was lowered, both the iron–ruthenium hybrid hemoglobins exhibited relatively higher cooperativity and a Raman line typical of normal deoxy structure, suggesting that their structure is stabilized at a "T-like" state. However, the oxygen affinity of $\alpha(Fe)_2\beta(Ru\text{-}CO)_2$ was lower than that of $\alpha(Ru\text{-}CO)_2\beta(Fe)_2$, and the transition to the "deoxy-type" Fe–N_ϵ stretching Raman line of $\alpha(Fe_2)\beta(Ru\text{-}CO)_2$ was completed at pH 7.4, while that of the complementary counterpart still remained in an "oxy-like" state under the same condition. These observations clearly indicate that the β-liganded hybrid has more "T"-state character than the α-liganded hybrid. In other words, the ligation to the α subunit induces more pronounced changes in the structure and function in Hb than the ligation to the β subunit. This feature agrees with our previous observations by NMR and sulfhydryl reactivity experiments. The present results are discussed in relation to the molecular mechanism of the cooperative stepwise oxygenation in native human adult hemoglobin.

In spite of a large number of investigations during the last several decades, the molecular mechanism of cooperative oxygen binding by hemoglobin (Hb)[1] is not yet fully understood. The cooperativity arises from the reversible transition between fully oxygenated and deoxygenated forms of human normal adult hemoglobin (Hb A), whose structures have been elucidated by X-ray crystallography [for example, see Baldwin (1980), Shaanan (1983), and Fermi et al. (1984)]. One of

† This work was supported by research grants from the Ministry of Education, Science and Culture of Japan (62220018 and 62790145).
* Author to whom correspondence should be addressed.
‡ Kyoto University.
§ Osaka University.

[1] Abbreviations: Hb A, human adult hemoglobin; NMR, nuclear magnetic resonance; Bis-Tris, [bis(2-hydroxyethyl)amino]tris(hydroxymethyl)methane; Tris, tris(hydroxymethyl)aminomethane; Ru-DPIXCO, ruthenium(II) carbonyldeuteroporphyrin; IHP, inositol hexakisphosphate.

0006-2960/89/0428-8603$01.50/0